

Superconductor-insulator transition in thin films driven by an orbital parallel magnetic field effect

Dganit Meidan¹ and Yuval Oreg^{1,2}¹*Department of Condensed Matter Physics, Weizmann Institute of Science, Rehovot 76100, Israel*²*Department of Applied Physics, Stanford University, Stanford, California 94305-4090, USA*

(Received 7 May 2009; published 12 June 2009)

We study theoretically orbital effects of a parallel magnetic field applied to a disordered superconducting film. We find that the field reduces the phase stiffness and leads to strong quantum phase fluctuations driving the system into an insulating behavior. This microscopic model shows that the critical field decreases with the sheet resistance, in agreement with recent experimental results. The predictions of this model can be used to discriminate spin and orbital effects. We find that experiments conducted by A. Johansson *et al.* are more consistent with the orbital mechanism.

DOI: [10.1103/PhysRevB.79.214515](https://doi.org/10.1103/PhysRevB.79.214515)

PACS number(s): 74.78.-w, 74.20.-z, 74.40.+k

I. INTRODUCTION AND RESULTS

Applying a magnetic field to a disordered superconducting film can drive it into a strong insulating state. This was observed both when the film is placed perpendicular to the field, in InO,¹⁻³ MoGe,⁴ TiN,⁵ and NbSe,⁶ or when the film is in parallel to the field orientation in InO (Refs. 7 and 8) and Bi.⁹ While several theoretical models support a superconductor-insulator transition in the perpendicular orientation,^{10,11} the mechanism that drives the transition when the field is parallel to the film remains unclear.

We study analytically a microscopic model of a disordered superconducting film with magnetic field applied *parallel* to the film, focusing on the induced orbital effects. We show that the field reduces the stiffness of the superconducting phase, leading to strong quantum phase fluctuations manifested as an insulating behavior. We find that the transition to the insulating phase occurs at a critical field that depends on the superconducting coherence length, ξ_0 , the film's thickness, d , and the sheet resistance, R_\square [see Eq. (1)]. We will show that this relation does not depend on the detailed mechanism that drives the transition, that it allows to determine experimentally if spin or orbital effects are dominant in parallel field, and that the measurements of Johansson *et al.*⁸ are more consistent with the orbital mechanism.

The emergence of a superconductor-insulator transition in disordered films induced by a *perpendicular* magnetic field is consistent with several theoretical scenarios. A *perpendicular* magnetic field penetrates the film in the form of vortices. As the field increases, these vortices were predicted to delocalize and Bose condense leading to an insulating behavior.¹⁰ Conversely, when the field is applied parallel to the film there are no field-induced vortices. An alternative numerical work studied the effect of thermal phase fluctuations in a disordered two-dimensional (2D) superconductor.¹¹ The *perpendicular* magnetic field was shown to destroy phase correlations between superconducting islands.¹²⁻¹⁶ Conversely, a *parallel* spin-exchange field causes the order-parameter phase and amplitude to vanish abruptly. While existing theories can account for the qualitative behavior seen in the *perpendicular* field orientation, they do not explain the surprisingly similar observed phenomenology when the field

is *parallel* to the film.⁷⁻⁹

We study the previously disregarded orbital effect of a *parallel* magnetic field applied to a disordered superconducting film. We find that the field uniformly decreases the superconducting order parameter and reduces its phase stiffness. The reduced phase stiffness enhances quantum fluctuations of the phase and amplitude, and can drive a quantum phase transition manifested as an insulating behavior. Our main prediction is that the critical field B_c that marks the onset of the insulating behavior depends on the critical temperature T_c , the film's sheet resistance, R_\square and thickness d as

$$\frac{B_c^2}{\tilde{H}^2} = \frac{1}{2} \left\{ \ln \left(\frac{R_Q}{R_\square} \right) - \ln 2K_0^c \right\}, \quad (1)$$

where $\tilde{H}^2 = \frac{12T_c\phi_0^2\nu_0}{\pi\gamma d} \frac{\Delta_0(B)R_\square}{\Delta_0 R_Q}$, $\gamma=1.78$, $\phi_0=hc/2e$ is the flux quantum, ν_0 is the density of states, $R_Q=h/(4e^2)$ is the resistance quantum, $\Delta_0(B)$ is the mean-field order parameter in the presence of a pair breaking field,¹⁷ and K_0^c is the critical value of the stiffness coefficient. Three points should be stressed herein. First, while the insulating behavior can be a result of either the proliferation of topological phase excitations, or of strong Gaussian phase fluctuations, the detailed mechanism that drives the transition will merely change the numerical factor K_0^c , as long as dissipation in the cores is negligible.^{18,19} Second, we do not consider the effects of a spin-exchange field, as some of the materials that exhibit the superconductor-insulator transition, such as MoGe, NbSe, and Bi, are expected to have strong spin-orbit scattering, which would smear spin-polarization effects. In addition, previous numerical work studied the effect of a spin-exchange field on thermal fluctuations in a nonuniform 2D superconductor.¹¹ In the absence of a perpendicular field, the amplitude and phase of the order parameter were shown to vanish abruptly with increasing spin-exchange field, indicating a transition into a metallic spin-polarized state,²⁰ contrary to the strong insulating behavior seen in experiments.^{7,8} However, while the spin mechanism is expected to depend on the thickness, d , only implicitly through T_c , the orbital critical field is inversely proportional to d . Hence, by studying the

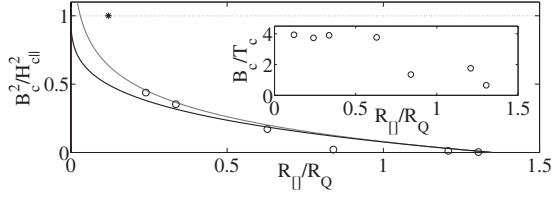


FIG. 1. Circles indicate the measured B_c^2 in units of $H_{c||}^2 = (1.6)^2 \phi_0^2 3T_c \nu_0 / (\gamma d) R_{\square} / R_Q$ versus the normalized resistance per square, R_{\square} / R_Q , taken from Ref. 8. Here T_c is obtained from an independent measurement. The clean sample of Ref. 8 (marked by an asterisk) exhibits a transition into a metal at high magnetic fields. We identify B_c in the cleanest sample with $H_{c||}$. The black and gray lines mark a fit of Eq. (1) to the data, for $\Delta(B_c)$ and $\Delta(B=0)$, respectively, using K_0^c and ν_0 as fitting parameters. K_0^c determines the maximal resistance films that exhibit a superconducting phase. The fitting values are $K_0^c = 0.37$, and $\nu_0 \sim 4.8 \times 10^{33} \text{ erg}^{-1} \text{ cm}^{-3}$. Estimates for K_0^c based on the proliferation of vortex loops give $0.46 < K_0^c < 0.75$ (see Fig. 3). ν_0 inferred from typical carrier densities in amorphous InO is $\nu_0 \approx 1.4 \times 10^{33} \text{ erg}^{-1} \text{ cm}^{-1}$. Inset: The measured B_c / T_c versus R_{\square} / R_Q . A transition driven by spin-exchange effects would imply that the ratio B_c / T_c be independent of R_{\square} . Here, we find a large scattering of the data. Moreover, in the presence of spin-orbit scattering, increasing the disorder (large R_{\square}) would enhance spin-orbit scattering, resulting in a larger B_c , whereas the data of Ref. 8 show the opposite tendency.

dependence of B_c field on the parameters of the system such as R_{\square} , d , and T_c , one can determine which mechanism dominates the transition. Finally, we find that the data of Ref. 8 is more consistent with Eq. (1) (see Fig. 1).

To gain insight to how the reduced stiffness can lead to an insulating behavior we consider as an example its effect on quantum vortex excitations, corresponding to a vortex loop in the three-dimensional (3D) classical analog of the system [see the discussion following Eq. (6) regarding the mapping the quantum 2D system onto a 3D classical system]. The energy cost of a circular vortex loop is $E_{\text{loop}} \sim E_{\text{core}} L / \xi + E_J L / \xi \ln L / \xi$, where E_{core} is the energy per unit length to suppress the gap in the core of the vortex and E_J is the energy per unit length to rotate the superconducting phase, and is determined by the phase stiffness. The logarithmic divergence in the rotational energy term will be cutoff for more complicated loop shapes. The entropy of a loop is determined by counting all possible configurations. On a cubic lattice this can be estimated by $S_{\text{loop}} \sim \ln(2D-1)^{L/\xi} \sim L/\xi$. A parallel magnetic field will reduce the core and rotational energies of the vortex loops [see derivation leading to Eq. (4)], leaving the entropy unchanged. As a result, vortex excitations become increasingly favorable and proliferate at a critical field which, in the absence of dissipation inside the vortex cores,^{18,19} marks the onset of the insulating behavior. In addition to its effects on topological excitations, the reduced phase stiffness also enhances Gaussian fluctuation of the superconducting phase. Loss of phase rigidity due to strong Gaussian fluctuations give similar estimates for the transition field as in Eq. (1), differing by a numerical factor K_0^c .

Figure 1 compares B_c calculated using Eq. (1) with the data of Ref. 8. The theoretical curve was plotted with K_0^c and

ν_0 used as fitting parameters. The microscopic model used to obtain Eq. (1) is valid in the disordered limit, for small pair breaking fields $B_c / H_{c||} < 1$. The clean sample of Ref. 8 exhibits a transition into a metal at high magnetic fields. We identify B_c in the cleanest sample with $H_{c||}$ (see asterisk in Fig. 1). While our theory is not applicable to the clean sample, we use this point to determine the relation between $H_{c||}$, T_c , and R_{\square} . The resulting $H_{c||} = 1.6 \sqrt{\frac{3}{8\pi}} \frac{\phi_0}{\xi_0 d} = 1.6 \phi_0 \sqrt{3 \frac{T_c \nu_0 R_{\square}}{\gamma d R_Q}}$ is larger than the critical field calculated in Ref. 17 by a factor 1.6. This may be a result of the finite thickness of the films used in Ref. 8. The inset of Fig. 1 shows the scaling of the measured B_c with the critical temperature T_c , as expected for a spin mechanism.²¹ We find that the data of Ref. 8 is more consistent with Eq. (1) (see caption of Fig. 1). We have tried to fit the experimental data of Ref. 9 to our model. B_c obtained using Eq. (1) is in better agreement with the experimental data than the critical field obtained from a linear $B_c \propto T_c$ or a square-root dependence $B_c \propto \sqrt{T_c}$, as naively expected from a spin mechanism, with weak or strong spin-orbit scattering, respectively. However, as apposed to InO,⁸ the distinction between the two mechanisms in Bi (Ref. 9) is quantitative rather than qualitative.

II. MODEL

We study the orbital effects of a parallel magnetic field on the low-energy excitations of the superconducting film. We consider the microscopic action of a quasi-2D superconducting film in the presence of a parallel magnetic field, obtained from the BCS Hamiltonian by a Hubbard-Stratanovich transformation followed by an expansion around the saddle point.²² Close to the critical temperature, in the limit $\Delta_0 \ll \omega, Dq^2 \ll T$, the action obtained in this way is the time-dependent Ginzburg Landau. Conversely, in the low-temperature limit, $T \ll \omega, Dq^2 \ll \Delta_0$, this yields²³⁻²⁶

$$\mathcal{S} = \nu_0 \Delta_0(B)^2 \int d\tau dx dy \int_{-d/2}^{d/2} dz \left\{ \frac{\rho^2}{2} [\ln \rho^2 - 1] + \xi_0^2 (\nabla \rho)^2 + \left(\frac{\partial_t \rho}{v_\rho} \right)^2 + 2\xi_0^2 \rho^2 \left[\left(\nabla \phi - \frac{2e}{c} A \right)^2 + \left(\frac{\partial_\tau \phi}{v_\phi} \right)^2 \right] \right\}, \quad (2)$$

where d is the film thickness, $v_\rho = \sqrt{(3\pi/2)D\Delta_0}$ is the amplitude velocity, $v_\phi = \sqrt{\pi D \Delta_0 (2dV_c \nu_0 + 1)}$ is the phase velocity, $\xi_0^2 = \pi D / 8 \Delta_0$, $V_c \approx 2\pi e^2 d$ is the Fourier transform of the short-range Coulomb interaction due to external screening, ν_0 is the density of states, D is the electronic diffusive constant, and the superconducting order parameter is parameterized as $\Delta(B) = \Delta_0(B) \rho e^{i\phi}$, with $\Delta_0(B)$, the mean-field solution, in the presence of the pair breaking parallel field.¹⁷

We ignore dynamic fluctuations of the electromagnetic field. This corresponds to assuming an infinite penetration depth of the magnetic field, and valid in the limit of very thin films. In the London gauge the uniform part of Eq. (2) is

$$\mathcal{S}_{\text{uni}} = \nu_0 d \Delta_0^2(B) \int d^2 r d\tau \left\{ \frac{\rho^2}{2} [\ln \rho^2 - 1] + \rho^2 \frac{B^2}{\tilde{H}^2} \right\}, \quad (3)$$

where $\tilde{H}^2 = \frac{12\Delta_0(B)}{\pi D e^2 d^2}$. Taking $\rho = \alpha \rho'$, and choosing α to eliminate the third term in Eq. (3), we obtain

$$S = v_0 d \Delta_0(B)^2 e^{-2(B^2/\tilde{H}^2)} \int dx dy d\tau \left\{ \frac{\rho'^2}{2} [\ln \rho'^2 - 1] + \xi_0^2 \left[(\nabla \rho')^2 + \left(\frac{\partial \rho'}{v_\rho} \right)^2 \right] + 2 \xi_0^2 \rho'^2 \left[(\nabla \phi)^2 + \left(\frac{\partial \tau \phi}{v_\phi} \right)^2 \right] \right\}. \quad (4)$$

Minimizing Eq. (4) with respect to ρ' yields²⁶ $\Delta_{MF} = \Delta_0(B) e^{-B^2/\tilde{H}^2}$.

Motivated by existing theoretical models that stress the role of phase fluctuations as the cause of the insulating behavior,^{10,11} we concentrate on the phase action in Eq. (4). Rescaling the spatial and imaginary time coordinates as $r \rightarrow r \sqrt{\frac{\Delta_0(B)}{D}}$, and $z = \tau \Delta_0(B)$, respectively, the phase action of Eq. (4) can be written as

$$\mathcal{S}[\phi] = \frac{K_0}{2} \int d^2 r dz \left((\nabla \phi)^2 + \frac{(\partial_z \phi)^2}{N_\perp^2} \right), \quad (5)$$

where

$$K_0 = \frac{\pi v_0 d D}{2} e^{-\pi D e^2 B^2 d^2 / (6 \Delta_0(B))} = \frac{R_Q}{2 R_\square} e^{-2B^2/\tilde{H}^2}, \quad (6)$$

is the stiffness coefficient and $N_\perp = p_F d$ is the number of transverse channels. Here we have used $dV_c v_0 \sim e^2 d^2 m p_F = \frac{e^2}{v_F} (p_F d)^2 \approx (p_F d)^2$. The stiffness coefficient determines the action of twisting the phase of the order parameter. When $K_0 \gg 1$, the superconducting phase is rigid. When $K_0 \ll 1$ the phase is strongly fluctuating. Hence, there exists a critical value K_0^c that marks the onset of strong phase fluctuations, whose exact numerical value depends on the details of the transition. From Eq. (6), this implies a critical parallel magnetic field, given by Eq. (1).

Equation (5) and (6) show that the parallel magnetic field reduces the phase stiffness. As a result, thermal and quantum phase fluctuations are enhanced. Close to the critical temperature, or for a sufficiently large pair breaking field, $\Delta_0(B) \ll T$, thermal phase fluctuations dominate. In this limit the reduced phase stiffness can drive a Kosterlitz-Thouless phase transition. The large number of normal excitations in this limit would manifest as a metallic behavior in the disordered phase. In this manuscript, we restrict our analysis to small pair-breaking fields or sufficiently low temperatures, such that the condition $\Delta_0(B) \gg T$ is met. In this limit quantum phase fluctuations dominate and the reduced stiffness can drive a 3D XY transition (see discussion below). As normal excitations are scarce in this limit, the loss of phase coherence would result in an insulating behavior, in agreement with experimental observations.^{7,8}

III. ESTIMATE OF K_0^c

While the critical field in Eq. (1) depends on the details of the transition only through K_0^c , this numerical factor becomes increasingly important in the limit $R_\square \rightarrow R_Q$. Equation (1)

shows that K_0^c determines the limiting value of R_\square/R_Q for which $B_c \rightarrow 0$, and the superconducting phase disappears.

To estimate the value of K_0^c we study the partition function of the quantum-mechanical system whose low-energy excitations are described by Eq. (5). The partition function takes the form of a sum of imaginary time transition amplitudes.²⁷ In the path-integral formulation of quantum mechanics, these transition amplitudes are calculated by summing over all possible paths. The path is determined by specifying the state of the system in finely spaced imaginary time intervals. Since Eq. (5) describes the behavior of the system at time intervals $\delta\tau > 1/\Delta$, the quantum-mechanical partition function formulated in this way has the same form as a classical partition function of a three-dimensional layered system with interlayer separation of $\delta\tau \sim 1/\Delta$. Hence, the microscopic phase action of Eq. (5) is in the universality class of the anisotropic 3D XY model, where the anisotropy is a result of the renormalization of the phase velocity due to Coulomb interactions.

The system described by the 3D XY model undergoes a transition between an ordered phase (superconductor) and a strongly fluctuating phase (insulator). Different mechanisms can drive the system into a strongly fluctuating phase, including strong Gaussian fluctuations and the proliferation of topological excitations. Estimates based on the Lindeman criterion give K_0^c up to a numerical factor which is usually determined experimentally. A more accurate estimate can be done based on the proliferation of vortex loops, using a 3D generalization of the Kosterlitz-Thouless scaling procedure.²⁸⁻³¹ We note that the critical exponents inferred from the 3D XY model are consistent with few experimental results.⁹

Previous works calculated the critical stiffness, K_0^c , for a phase only 3D XY model, Eq. (5).^{30,31} The resulting K_0^c implies that films with $R_\square/R_Q > 0.64$ should not exhibit a superconducting phase. Conversely, the data of Ref. 8 show that a transition persists for $R_\square/R_Q \leq 1.31$. Moreover, the phase only model is applicable to inhomogeneous systems such as Josephson-junction arrays. In a homogenous system such as a superconducting film, however, a vortex excitation can only occur once the superconducting amplitude is locally suppressed. We solve the flow Eqs. (7) and (8), with corrected initial conditions to account for both the phase rotation and the amplitude suppression inside the vortex core [see the discussion following Eq. (8)]. The critical bare physical parameters are the initial conditions that flow to the critical point of Eq. (8). The microscopic action [Eq. (4)] allows to express these critical parameters in terms of measurable quantities, such as R_\square and B .

The large number of perpendicular channels, $N_\perp \gg 1$, in quasi-2D films generates a strong anisotropy between the spatial dimension and the imaginary time dimension, Eq. (5). This strong anisotropy in the stiffness coefficient introduces a crossover scale $a' = \xi_0 N_\perp$. The scaling of the phase stiffness and vortex loop fugacity in the 3D XY model can be obtained in two regimes. At small distances $a < a'$, dominant excitations are found to be rectangular loops, cutting single planes

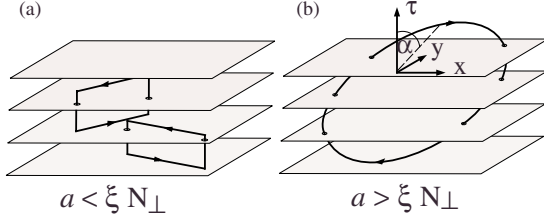


FIG. 2. (Color online) The critical bare stiffness was calculated assuming: (a) quasi-2D rectangular loops (Ref. 32) at scales $a < \xi N_{\perp}$, and (b) multiplane loops at scales $a > \xi N_{\perp}$.

[Fig. 2(a)].³² The scaling equations at these scales are quasi-2D,³¹

$$\frac{dK_l^{2D}}{dl} = -4\pi^3 K_l^{2D} y_l^{2D},$$

$$\frac{dy_l^{2D}}{dl} \approx \left[4 - 2\pi K_l^{2D} \left(1 + U(0) N_{\perp}^{-2} \frac{e^l}{2} \right) \right] y_l^{2D}, \quad (7)$$

where $l = \ln a$ is the running scale, and K_l^{2D} and y_l^{2D} are the quasi-2D renormalized stiffness and fugacity, respectively. Here $U(0) = \sum_{q,\omega} 4\pi / (q^2 + \omega^2 / N_{\perp}^2)$ is the phase propagator, and the sum is cutoff at the effective core size that accounts for the crinkling of the vortex loops.³¹ At larger distances $a > a'$ the system is no longer sensitive to the anisotropy, and dominant excitations are multiplane vortex loops [Fig. 2(b)]. In this regime, the renormalized $K_{l'}^{2D}$ and $y_{l'}^{2D}$ of Eq. (7) at $l' = \ln(a'/a)$ are used as initial conditions for the isotropic scaling equations for multiplane loops,³⁰

$$\frac{dK_l}{dl} = K_l - \frac{4\pi^3}{3} y_l K_l^2,$$

$$\frac{dy_l}{dl} = [6 - \pi^2 K_l (1 - x \ln K_l)] y_l. \quad (8)$$

Here $x=0.6$ is the self-avoiding random-walk exponent. It accounts for partial cancellation of the Biot-Savart-type interaction in complicated loop geometries.^{30,33}

We calculate the initial conditions of Eq. (7) for a homogeneous system, with both phase and amplitude fluctuations. The bare value of the stiffness coefficient is³¹ $K_0^{2D} = K_0 / [1 + (2K_0)^{-1}]$, with K_0 given by Eq. (6). The bare fugacity of a vortex loop is $y_0^{2D} = \exp\{-S_j - S_c\}$, where S_j and S_c are the a self-rotational and core actions, respectively. Previous works calculated S_j for a phase only model.³¹ The self-rotational action of the smallest rectangular loop was found to be $S_j = \pi^2 K_0 / [1 + (2K_0)^{-1}]$. Here we add an estimate for S_c , calculated from Eq. (4), using a variational method. The anisotropy between the spatial dimension and the imaginary time dimension introduces two possible excitations: a vortex, manifested as a rotation of the phase in the x - y plane, and a phase slip which is the corresponding rotation in the x - τ or y - τ planes. A vortex loop in the $2+1$ -dimensional world is a complicated combination of vortex and phase slips segments. To calculate the core action of such a multiplane excitation, we first determine the action of vortex core of unit volume

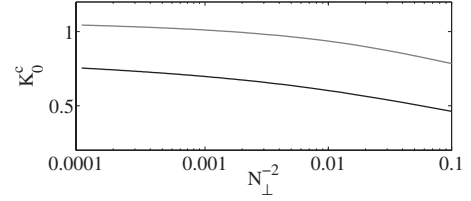


FIG. 3. The critical stiffness, K_0^c , versus the anisotropy parameter, $N_{\perp}^{-2} = \frac{1}{(\rho_r d)^2}$, calculated using Eqs. (7) and (8), with the corrected initial conditions including both amplitude and phase fluctuations (black curve) and the phase only initial conditions (gray curve). We find that K_0^c derived for the phase and amplitude initial conditions is more consistent with the experimental data of Ref. 8 [see discussion following Eq. (8)].

r_0^2 / Δ_{MF} , and of a phase slip of unit volume $r_0 \xi_0 / \Delta_{MF}$. We choose the following trial function for a phase slip and a vortex, respectively:

$$\phi_{ps} = \arctan\left(\frac{v \phi \tau}{x}\right), \quad \rho_{ps} = \min\left[\sqrt{\left(\frac{x}{r_0}\right)^2 + (\tau \Delta_{MF})^2}, 1\right],$$

$$\phi_v = \arctan\left(\frac{y}{x}\right), \quad \rho_v = \min\left[\sqrt{\frac{x^2 + y^2}{r_0^2}}, 1\right]. \quad (9)$$

Identifying the part of the action [Eq. (4)] that corresponds to $\rho \neq 1$ as the core action, we minimize this expression with respect to the core size, r_0 . The resulting core actions of unit volume are

$$S_c^{ps} = K_0 \left(\sqrt{\frac{\pi}{6}} + \frac{\pi}{2} \frac{1}{N_{\perp}} \right),$$

$$S_c^v = K_0 \left(\frac{1 + 3\pi}{4} \right), \quad (10)$$

where K_0 is given by Eq. (6). In quasi-2D films with $N_{\perp} \gg 1$, rectangular loops dominate.³² The smallest rectangular loop has ξ_0 unit sides of circulation segments in the τ direction and $2\xi_0$ sides of circulation pointing in the x - y plane. As a result, the bare core action of a rectangular loop is $S_c = 2S_c^v + 4S_c^{ps}$.

The bare critical stiffness, $K_0^c(N_{\perp})$, identified as the initial condition derived for the phase and amplitude model [Eq. (4)] that flow to the critical point of Eq. (8) is plotted in black in Fig. 3. The same quantity calculated for a phase only model is plotted in gray. The initial conditions corresponding to phase and amplitude fluctuations give $0.46 < K_0^c(N_{\perp}) < 0.75$, for $10 < N_{\perp}^2 < 10^4$. This implies that for the physically realized values of N_{\perp} a transition could occur up to $R_{\square}/R_Q \leq 1.08$, compared to $R_{\square}/R_Q \leq 0.64$ found for the phase only model. Hence, the estimates for $K_0^c(N_{\perp})$ based on the phase and amplitude model are more consistent with the data of Ref. 8 that show a transition in samples with $R_{\square}/R_Q \leq 1.31$. Our estimates of S_c neglected the possible crinkling of the vortex loops. These would result in a larger core action, and therefore a larger range of R_{\square}/R_Q that exhibit a transition.

IV. SUMMARY

We study the previously disregarded orbital effect of a magnetic field applied parallel to a superconducting film. We find that the parallel field reduces the phase stiffness and leads to strong phase fluctuation at a critical magnetic field that depends on the film's sheet resistance, Eq. (1). This prediction does not depend on the details of the transition, it allows to experimentally determine if spin or orbital effects drive the transition in the parallel orientation, and it shows that the data of Ref. 8 are more consistent with the orbital mechanism (see Fig. 1). A quantitative estimate for the transition field depends on the detailed process by which strong phase fluctuations lead to an insulating behavior. In this manuscript we consider as an example the proliferation of topological excitations as a possible mechanism. We map the microscopic action of the 2D film onto the 3D XY model. By

solving the scaling equations derived for the 3D XY model³¹ with corrected initial conditions to account for both amplitude and phase fluctuations, we get a better agreement with the data of Ref. 8. We note that the phenomenology of an insulating behavior induced by strong phase fluctuations can be generalized to other mechanisms that reduce the phase stiffness in a continuous fashion including impurity concentration and changing the thickness, as long as dissipation in the cores can be neglected.

ACKNOWLEDGMENTS

We would like to acknowledge useful discussions with E. Altman and G. Refael. We thank K. A. Parendo, K. H. Sarwa, A. Goldman, A. Johansson, and D. Shahar for letting us use their data. This paper was supported by an ISF and a DIP grant.

-
- ¹A. F. Hebard and M. A. Paalanen, Phys. Rev. Lett. **65**, 927 (1990).
²V. F. Gantmakher, M. V. Golubkov, V. T. Dolgoplov, G. E. Tsydynzhapov, and A. A. Shashkin, Pis'ma Zh. Eksp. Teor. Fiz. **71**, 231 (2000) [Sov. JETP Lett. **71**, 160 (2000)].
³G. Sambandamurthy, L. W. Engel, A. Johansson, and D. Shahar, Phys. Rev. Lett. **92**, 107005 (2004).
⁴A. Yazdani and A. Kapitulnik, Phys. Rev. Lett. **74**, 3037 (1995).
⁵T. I. Baturina, D. R. Islamov, J. Bentner, C. Strunk, M. R. Baklanov, and A. Satta, Pis'ma Zh. Eksp. Teor. Fiz. **79**, 416 (2004) [Sov. JETP Lett. **79**, 337 (2004)].
⁶H. Aubin, C. A. Marrache-Kikuchi, A. Pourret, K. Behnia, L. Berge, L. Dumoulin, and J. Lesueur, Phys. Rev. B **73**, 094521 (2006).
⁷V. F. Gantmakher, M. V. Golubkov, V. T. Dolgoplov, A. A. Shashkin, and G. E. Tsydynzhapov, Pis'ma Zh. Eksp. Teor. Fiz. **71**, 693 (2000) [Sov. JETP Lett. **71**, 473 (2000)].
⁸A. Johansson, N. Stander, E. Peled, G. Sambandamurthy, and D. Shahar, arXiv:0602160 (unpublished).
⁹K. A. Parendo, K. H. Sarwa B. Tan, and A. M. Goldman, Phys. Rev. B **73**, 174527 (2006).
¹⁰M. P. A. Fisher, Phys. Rev. Lett. **65**, 923 (1990).
¹¹Y. Dubi, Y. Meir, and Y. Avishai, Nature (London) **449**, 876 (2007).
¹²The interplay between strong disordered and strong magnetic field was found to introduce spatial fluctuations in the superconducting gap. See for example Ref. 13–16.
¹³F. Zhou and B. Spivak, Phys. Rev. Lett. **80**, 5647 (1998).
¹⁴A. Ghosal, M. Randeria, and N. Trivedi, Phys. Rev. Lett. **81**, 3940 (1998).
¹⁵V. M. Galitski and A. I. Larkin, Phys. Rev. Lett. **87**, 087001 (2001).
¹⁶A. Ghosal, M. Randeria, and N. Trivedi, Phys. Rev. B **65**, 014501 (2001).
¹⁷K. Maki, *Gapless Superconductivity* (Dekker, New York, 1969), Chap. 18.
¹⁸We neglect dissipation inside the cores of quantum vortices since the density of states of a dirty *s*-wave SC is expected to be suppressed around the fermi energy, with an energy gap of $\delta \approx \Delta R_{\square}/R_Q$ (Ref. 19).
¹⁹R. Bundschuh, C. Cassanello, D. Serban, and M. R. Zirnbauer, Nucl. Phys. B **532**, 689 (1998).
²⁰A. M. Clogston, Phys. Rev. Lett. **9**, 266 (1962).
²¹Corrections to the critical spin-exchange field due to mesoscopic fluctuations were calculated in Ref. 13.
²²The expansion is done in the dirty limit, $\Delta_0 \tau \ll 1$, where τ is the scattering mean free time.
²³U. Eckern and F. Pelzer, J. Low Temp. Phys. **73**, 433 (1988).
²⁴R. A. Smith, M. Y. Reizer, and J. W. Wilkins, Phys. Rev. B **51**, 6470 (1995).
²⁵A. van Otterlo, D. S. Golubev, A. D. Zaikin, and G. Blatter, Eur. Phys. J. B **10**, 131 (1999).
²⁶D. Meidan, Y. Oreg, G. Refael, and R. A. Smith, Physica C **468**, 341 (2008).
²⁷S. L. Sondhi, S. M. Girvin, J. P. Carini, and D. Shahar, Rev. Mod. Phys. **69**, 315 (1997).
²⁸D. R. Nelson and D. S. Fisher, Phys. Rev. B **16**, 4945 (1977).
²⁹G. A. Williams, Phys. Rev. Lett. **59**, 1926 (1987).
³⁰S. R. Shenoy, Phys. Rev. B **40**, 5056 (1989).
³¹S. R. Shenoy and B. Chattopadhyay, Phys. Rev. B **51**, 9129 (1995).
³²S. Hikami and T. Tsuneto, Prog. Theor. Phys. **63**, 387 (1980).
³³B. Chattopadhyay, M. C. Mahato, and S. R. Shenoy, Phys. Rev. B **47**, 15159 (1993).